

Using a Carbon Black for the Lead Powder Preparation from the Lead Paste by Calcination and Its Application as Positive Lead Plate for Lead Acid Battery

Keqiang Ding^{1,3,*}, Xiaojing Gao¹, Jingwei Han¹, Chenxue Li¹, Xiaomi Shi¹, Hui Wang³, Hongmin Dou³, Zhigang Guo⁴, Yu Liu⁴, Junqing Pan^{2*}

¹ College of Chemistry and Materials Science, Hebei Normal University, Shijiazhuang 050024, P.R. China

² State Key Laboratory of Chemical Resource Engineering, Beijing Engineering Center for Hierarchical Catalysts, Beijing Advanced Innovation Center for Soft Matter Science and Engineering, Beijing University of Chemical Technology, Beijing, 100029, P.R. China

³ Hebei LingDian New Energy Technology Co., Ltd, Tangshan, Hebei, 064200, P.R.China

⁴ Tianneng Battery Group Co., Ltd. Changxing, Zhejiang, 313100, P.R.China

To whom the correspondence should be made:

*E-mail: dkeqiang@263.net; jqpan@mail.buct.edu.cn

Received: 4 September 2018 / Accepted: 24 October 2018 / Published: 30 November 2018

In this work, the worn-out lead pastes of the seriously softened positive lead plates of a lead acid battery are, for the first time, successfully recovered to be lead powder using a facile method of carbon black-present calcination. Namely, the mixtures containing the worn-out lead pastes and carbon black are calcined at 400 °C for 5 h, and the resultant samples with a carbon black content (mass ratio) of 0.3%, 0.6%, 1.2% and 3.1% in the starting materials are labeled as sample a, b, c and d, respectively. The results of XRD patterns reveal that the main component of the worn-out lead pastes is β -PbO₂, and after the calcination treatment, Pb-based oxides with relatively lower Pb chemical valence are demonstrated to be the major ingredients of all prepared samples. SEM images strongly indicate that the content of carbon black in the starting materials is a main factor which can greatly influence the morphologies of the resultant samples, and more smaller and rod-shaped particles are displayed in sample b. More importantly, the discharge capacity of sample b is maintained as high as 458 mAh, being very close to that of the fresh industrial lead powder (468 mAh).

Keywords: lead acid battery; carbon black; calcination; lead powder recycling

1. INTRODUCTION

Besides the separator and sulfuric acid solution, a lead acid battery (briefed as LAB) is mainly constructed by a negative lead plate and a positive lead plate. And generally, prior to the formation

process, the negative lead plate is a lead grid which is fully coated by the negative lead paste, and the positive lead plate is a positive lead paste-coated lead grid. After the formation process, the negative lead plate mostly becomes an elementary Pb coated lead grid, and the positive lead plate is converted to be a PbO₂-coated lead grid. Thus, Pb is the main element of a commercial LAB [1, 2]. Recently, the sharp increase in the quantity of both vehicles (mainly including fuel vehicles and electric vehicles) and electric bicycles has enormously stimulated the market development of lead acid batteries. Therefore, lead, only next to aluminum, has become the second-largest consumed metal in the world [3]. It is well known that lead is a toxic and non-renewable metal, thus, how to recover lead from the worn-out lead acid batteries has turned into a critical project for the lead acid battery-related researchers [4].

Generally speaking, the recovered lead was mainly originated from both the current collector (namely, the lead grid of a LAB) and the worn-out lead paste of a LAB. Evidently, it is easy to recover lead from the lead grid since almost no consumption of lead grid was found for all worn-out lead acid batteries. And, recovering lead from the worn-out lead paste was a very difficult issue because of the fact that the worn-out lead paste was a mixture rather than a pure substance due to the presence of some additives. Of late, the recovery of lead from the worn-out lead acid batteries has been widely carried out mainly owing to the urgent demand of both lead consumption in industry and the reduction of lead pollution. For example, a hydrogen-lead oxide fuel cell based green hydrometallurgical process for recovering lead was developed by Pan's group [5], and in their works, metallic Pb was recovered by an electrochemical reduction reaction of $\text{PbO(s)} + 2\text{e}^- + \text{H}_2\text{O} + \text{OH}^- \rightarrow \text{Pb(s)} + 3\text{OH}^-$. And it should be emphasized that PbO used in their works was obtained using a desulfurization process of lead sulphate from the spent lead paste of the used LABs. Volpe and his coworkers [6] developed a new way for recovering metallic lead from the worn-out lead paste, namely, PbO and PbSO₄ in the lead paste firstly were dissolved in urea acetate to form a solution, and then the formed Pb(Ac)₂ reacted with metallic iron to prepare the metallic lead. Mirza's group [7], through developing a recovery and refining process, systematically explored how the recycled lead became the material for battery construction. In their works, the process for refining the secondary lead majorly included battery breaking and component separation, sulfur removal, smelting and refining processes. Except for above works focusing on the recovery of metallic lead, the recovery of lead oxide was also conducted in recent years. In 2016, Pan's group [8] developed a method for the direct recovery of lead oxide (PbO) from the waste lead pastes and lead grids of the spent lead-acid batteries. And in his work, the lead pastes and lead grids were firstly converted into PbSO₄ totally, and then, after the desulfurization and recrystallization processes α -PbO was successfully prepared. Although the recovery research of metallic lead and lead oxide has been carried out in above works, to the best of our knowledge, this is no paper reporting the recovery of the lead powder from the worn-out lead pastes of the seriously softened positive lead plates (SSPLP) using a carbon black-present calcination process.

What is the so-called SSPLP? How do they come into being? By the naked eye, the lead paste of the SSPLP looks like red mud which can be easily scraped from the SSPLP. For a LAB with the SSPLP, it can be fully charged in a very short period, and in the practical application, the fully charged LAB shows a very rapid electricity loss leading to the invalidity of a LAB. According to our practical experience, the failure of a lead acid battery was basically resulted from the following reasons: (1) Exceeding the usage life of a LAB; (2) The exfoliation of the lead paste from the lead grid due to the

severe mechanical vibration under some special conditions; (3) The inactivation of the lead paste chiefly owing to the irrational use of a LAB; (4) Man-made damage of a LAB; (5) The softening of the positive plate of a LAB. Amongst as-mentioned reasons, the issue of the positive lead plate softening is the most difficult problem which has not yet been well resolved, mainly because of the fact that the reasons for the softening of the positive lead plate still remained suspended. Generally known, the use time of a worn-out LAB with the SSPLP was very short, thus, most parts of the worn-out LAB with the SSPLP were nearly-new which should be well recovered for the further cyclic utilization. To our knowledge, up to now, this is no paper reporting the recovery of the lead powder from the lead paste of the SSPLP using a carbon black -present calcination process.

In this work, firstly, the lead paste was carefully scraped from the SSPLP, and after a careful cleaning and drying, the well milled lead paste was thoroughly mixed with carbon black to generate a mixture. And then, the mixture with various contents of carbon black was calcined at 400 °C for 5 h leading to the formation of four final samples. And the produced samples were thoroughly characterized by XRD, SEM, FTIR and XPS. Lastly, the produced samples were used again as the lead powder to prepare the positive lead plates constructing a simulated lead acid battery, and the results of galvanostatic charge/discharge measurement inspiringly indicated that the discharge capacity of sample b was close to 90% of the fresh industrial paste. That is to say, carbon black-present calcination method was a feasible way to recover the lead powder from the worn-out paste of the SSPLP, which was very meaningful to the cyclic utilization of the obsolete lead acid batteries.

2. EXPERIMENTAL DETAILS

2.1 Reagents and materials

All chemicals were used as received without any further purification. All the battery materials, including the seriously softened positive lead plate, the fresh industrial lead powder, the lead grid as well as the additive agents used to produce a raw lead plate, were provided by the Tianneng Group. Both the lead paste preparation method and the battery formation process, being identical to those of the industrial processes for producing a commercial lead acid battery, were also offered by the Tianneng Group.

2.2 Preparation of the samples

Firstly, the lead paste was carefully scraped from the SSPLP (photo 4 in Fig.1), and then, the scraped paste was washed with distilled water for several times until the pH value of the filtrate was equal to 7. After that, the obtained samples were dried in an air dry oven at 80 °C for 4 h. Subsequently, the well cleaned and dried samples were thoroughly ground in an agate mortar for 30 min to produce the powdery samples. And then, the produced powdery samples were fully mixed with a proper amount of carbon black to produce a mixture, and lastly, the produced mixture was sintered in a muffle furnace at 400 °C for 5h to produce the final samples. The synthesized samples with the mass ratio of carbon black in the starting mixture before calcination of 0.3%, 0.6%, 1.2% and 3.1% were nominated as sample a, b,

c and d, respectively. For comparison, the fresh industrial positive lead powder and the lead paste directly scraped from the SSPLP were, respectively, called as sample o and s.

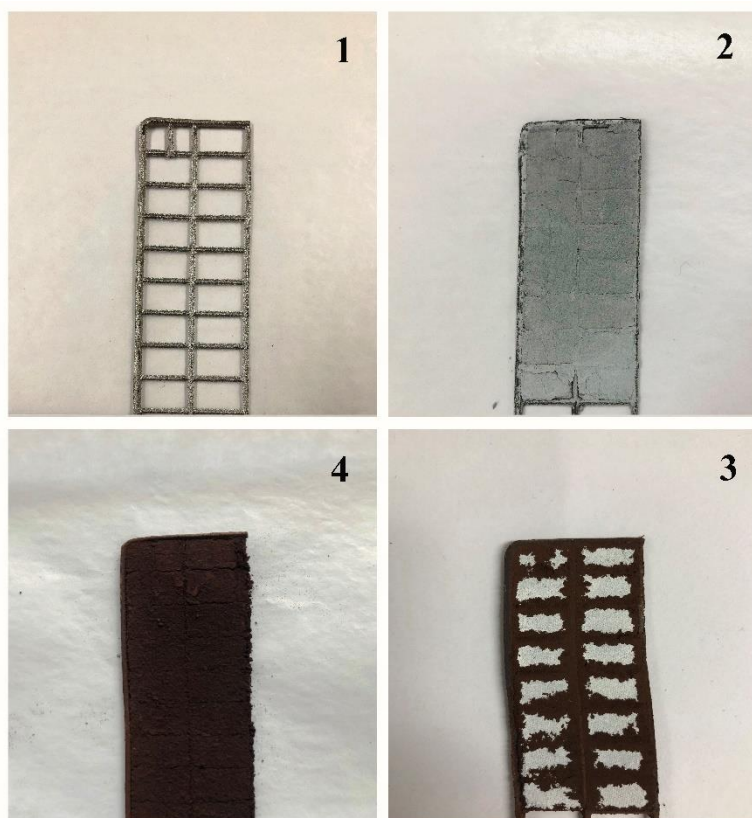


Figure 1. Photos for the materials used in this work. Photo 1: the lead grid; photo 2: the raw positive lead plate; photo 3: the matured positive lead plate; photo 4: the seriously softened positive lead plate (SSPLP)

2.3 Preparation of a simulated lead acid battery

The simulated lead acid battery was assembled by a positive lead plate and a negative lead plate. The positive lead plate was prepared based on the following process [9]. Namely, a certain amount of sulfuric acid with a density of 1.4 g cm^{-3} and a proper amount of fiber-contained distilled water were added into 25 g of one prepared sample which was followed by a thorough stirring, generating a wet lead paste. And then, the resultant wet lead paste was smeared on a positive lead grid generating a wet positive lead plate. It should be noticed that the size of the lead grid was $70 \text{ mm} \times 25 \text{ mm} \times 1 \text{ mm}$, and the weight of the wet lead paste on each lead grid was about 7 g. Subsequently, the wet positive lead plate was placed in air at room temperature for about 12 h, and soon afterwards, it was dried in an air dry oven at $80 \text{ }^\circ\text{C}$ for 2 h to produce the so-called positive raw lead plate.

The negative lead plate was fabricated using a similar preparation process. That is, 25 g of fresh industrial lead powder and a proper amount of additives (mainly including barium sulfate, lignin, carbon black and zinc oxide) were mixed together by a thorough stirring, and then, the obtained mixture was ground in an agate mortar for 30 min to form a new powder. And then, a proper amount of sulfuric acid

(1.4 g cm^{-3}) and a proper amount of fiber-contained distilled water were added into above resultant powder. Other processes were identical to those of the positive lead plate preparation.

The simulated lead acid battery was constructed by an as-prepared positive lead plate and a produced negative lead plate. And, the battery formation process of the simulated lead acid battery was carried out on an equipment of NEWARE in a sulfuric acid solution (1.05 g cm^{-3}), in which the battery formation current density applied (about 11 mA cm^{-2}) was calculated based on the empirical values provided by the Tianneng Group. After the formation process, the raw lead plates were converted into the so-called matured lead plates. That is to say, after the formation treatment, the main components of the positive lead paste and the negative lead paste were varied from PbO (the main component of the raw lead paste) to PbO₂ (the main component of the matured positive lead paste), and, from PbO to metallic Pb (the main component of the matured negative lead paste), respectively [10]. The discharge process of the charged lead acid battery was conducted using a constant current method in which the discharge current was calculated according to the empirical electric quantity of the fresh industrial lead powder (namely, the electric quantity of 1g fresh industrial lead powder was close to 100 mAh). The cut-off potentials for the charging and discharging processes were 2.4 V and 1.75 V, respectively. In each battery measurement, the negative lead plate, in terms of both material and preparation process, was kept identical to each other, and the positive lead plate changed correspondingly. Thus, the simulated lead acid battery assembled by sample o, s, a, b, c and d, were named as battery o, s, a, b, c and d, respectively.

The photos for some typical materials appearing in this work are shown in Fig.1. Photo 1 of Fig.1 was the photo for the lead grid. Generally, the lead grid was a metallic lead based alloy which also was called as current collector. The photo of the raw lead positive plate was presented by photo 2. While, after the formation process, as shown by photo 3 in Fig.1, a matured lead positive plate was produced which mainly consisted of the lead grid (black grid) and white lead paste. Photo 4 was the photo for the SSPLP, seen by the naked eye, being black red.

2.4 Characterization

X-ray diffraction (XRD, Bruker D8 ADVANCE X-ray diffractometer equipped with a Cu K α source ($\lambda = 0.154 \text{ nm}$) at 40 kV and 30 mA), Scanning electron microscopy (HITACHI, SEM S-570), Energy-dispersive X-ray spectroscopy (EDS, PV-9900, USA) and X-ray photoelectron spectroscopy (XPS, Kratos Analytical spectrometer, Al K α radiation) were used to examine the composition, morphology, element composition and the valence of the elements of the produced samples, respectively. The formation process and the charging process as well as the discharging process were all conducted on an equipment of CT-3008W-5V3A-S1(Neware Technology Limited, China).

3. RESULTS AND DISCUSSION

3.1 XRD analysis

To investigate the crystal structure and the compositions of the prepared samples, all the synthesized samples including the fresh industrial lead powder (sample o) and the lead paste scraped

from the SSPLP (sample s) were studied using XRD, and the results are illustrated in Fig.2a and 2b. Apparently, the XRD pattern of sample s matched well with the standard XRD pattern of β -PbO₂ (JCPDS: 00-041-1492) which strongly indicated that the main component of the SSPLP was β -PbO₂.

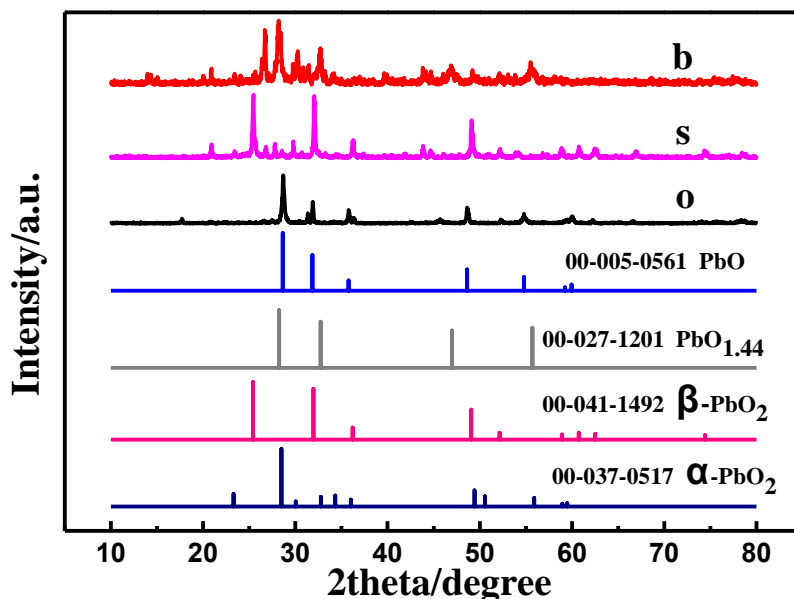


Figure 2a. XRD patterns for the involved materials. Pattern o, s and b corresponded to sample o, s and b. The standard XRD patterns for PbO, PbO_{1.44}, β -PbO₂ and α -PbO₂ were also presented.

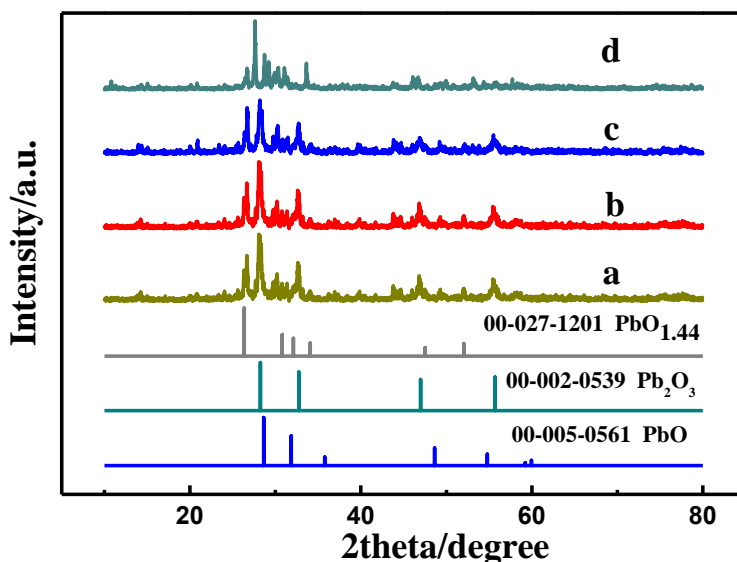


Figure 2b. XRD patterns for all prepared samples. Pattern a, b, c and d corresponded to sample a, b, c and d. The standard XRD patterns for PbO_{1.44}, Pb₂O₃ and PbO were also presented.

Also, the sharp diffraction peaks exhibited by pattern s evidenced a relatively higher crystallinity of the particles in sample s [11]. Meanwhile, the diffraction peaks for sample o corresponded well to the standard XRD pattern of PbO (JCPDS:00-005-0561), which effectively suggested that the main component of the fresh industrial lead powder was PbO. Interestingly, after the calcination process, the

main diffraction peaks assigned to PbO_2 , as shown by pattern b in Fig.2b, totally disappeared, and instead, the diffraction peaks corresponding to both $\text{PbO}_{1.44}$ (JCPDS:00-0137-0516) and Pb_2O_3 (JCPDS:00-002-0539) were displayed distinctly. This result strongly indicated that after the carbon black-present calcination treatment, most parts of PbO_2 in sample s have been successfully converted into lead oxides (with relatively lower Pb chemical valence). Also, it can be seen clearly that similar XRD patterns were displayed by all produced samples especially for sample a, b and c. This result substantially indicated that similar ingredients were contained in sample a, b and c. Summarily, XRD results shown in Fig.2a and 2b strongly demonstrated that the content of carbon black in the starting materials was a key factor which had a pivotal role in determining the compositions of the final samples, and, the developed carbon black-present calcination process was a feasible way to chemically reduce PbO_2 to be lead oxide with relatively lower Pb chemical valence.

3.2 Morphology characterization

Prior to the study of the micromorphology of the as-prepared samples, the photos for all the prepared samples were shown in Fig.3a. Clearly, as shown by photo o in Fig.3a, the fresh industrial lead powder was gray powder, and the lead paste scraped from the SSPLP was black red powder (photo s in Fig.3a).

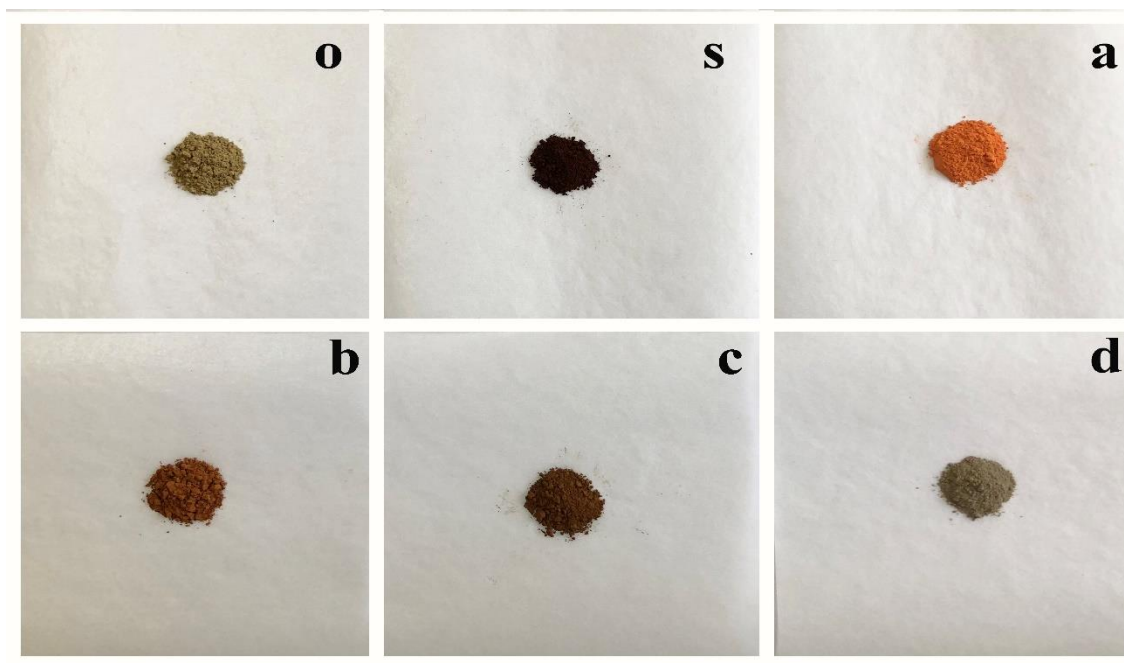


Figure 3a. Photos for the involved samples. Photo o, s, a, b, c and d corresponded to sample o, s, a, b, c and d.

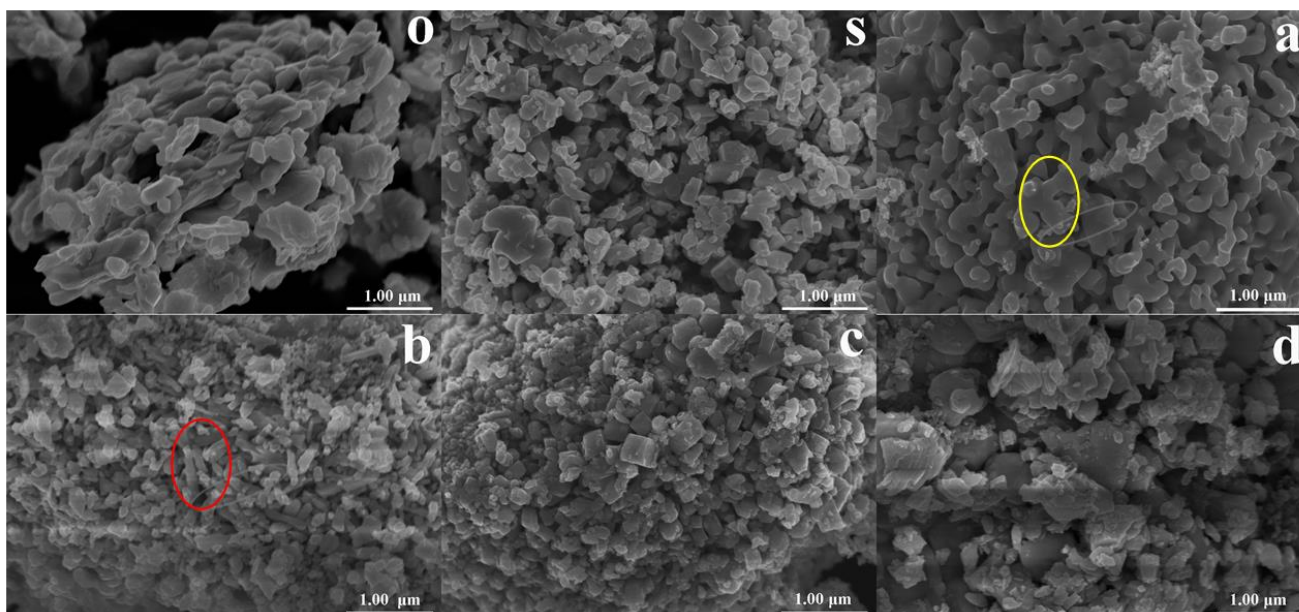


Figure 3b. SEM images for the involved samples. Image o, s, a, b, c and d corresponded to sample o, s, a, b, c and d.

Interestingly, for sample a, orange red powder was seen clearly, and sample b showed soil red color. And, due to the increase of carbon content in the starting materials, sample c and d showed dark soil red and gray color, respectively. Thus, it can be concluded that the content of carbon in the starting material (namely, the mixture having the carbon black and the lead powder scraped from the SSPLP) was an important factor which could affect the color of the produced samples. Also, the color variation of the synthesized samples strongly indicated that the compositions of the prepared samples were different from each other, being consistent with the fact that each sample had its own XRD pattern (Fig.2a and 2b).

The micromorphologies of all the involved samples were also characterized by SEM and the results are shown in Fig.3b. Evidently, the particles of sample o had irregular shapes and showed the largest particle size among all the produced samples. While, in the case of sample s, relatively regular and smaller particles with blocky-shape were exhibited clearly. After the calcination process, as shown by the yellow-circled part in image a, more larger and linked particles were displayed in sample a. Also, as shown by the red-circled parts in image b, some smaller and cylinder-shaped particles were seen clearly. It seemed, as shown by image c in Fig.3b, some cubic particles with different sizes were produced in sample c. When the carbon content in the starting material reached 3.1%, as illustrated by the image d in Fig.3b, some huge agglomerates were produced. The change in the morphologies of the prepared samples effectively indicated the composition variation of the resultant samples, which accorded well with the XRD pattern results shown in Fig.2a and 2b.

The N_2 adsorption-desorption isotherms of all involved samples were measured and compared in Fig.4a. The shapes of all curves were very similar to those of mesoporous hollow nanospheres consisting of carbon coated silica, which remarkably implied that all the prepared samples had a porous structure [12]. The pore volumes of sample a, b, c and d were roughly estimated to be 0.060, 0.062, 0.058 and 0.010 $cm^3 g^{-1}$, respectively. Generally, the larger pore volume of a material was beneficial to the

flowing of the electrolyte, and the higher specific surface area of an electrode material was advantageous to the increase in contacting area of between the electrode and the electrolyte. The specific surface areas of all the prepared samples were also calculated (The specific surface areas for sample a, b, c and d were respectively calculated to be 54.3, 13.4, 50.4 and 10.4 $\text{m}^2 \text{g}^{-1}$), and unfortunately, no regular data were obtained. This result, in turn, just documented that the battery performance exhibited by the prepared samples should be mainly determined by their chemical compositions rather than the physical properties like particle size. Therefore, the results of Fig.4a, at least, demonstrated that all the prepared samples had a porous structure which was very favorable to the contacting of between the electrode material and sulfuric acid solution.

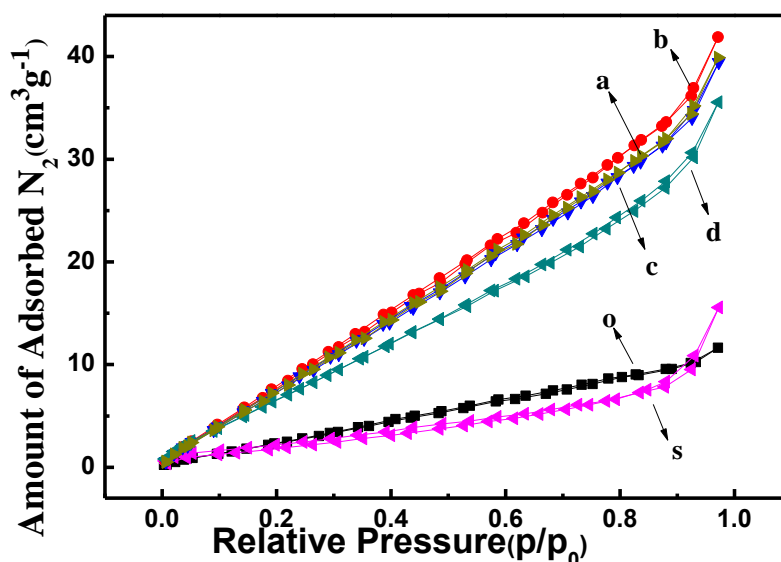


Figure 4a. Nitrogen adsorption-desorption isotherms of the involved samples. Curve o, s, a, b, c and d corresponded to sample o, s, a, b, c and d.

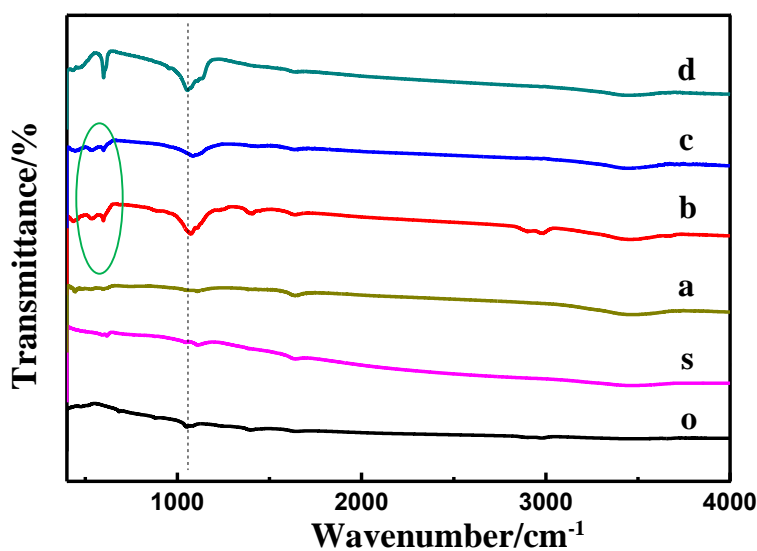


Figure 4b. FTIR spectra for all the samples. Curve o, s, a, b, c and d corresponded to sample o, s, a, b, c and d.

FTIR spectra of all involved samples were displayed in Fig.4b. For sample s, the weak bands at 1622.0 cm^{-1} and 3429.2 cm^{-1} (respectively corresponding to the C=O and -OH groups) were demonstrated to be mainly originated from the strong adsorption of CO_2 and H_2O on the surface of sample s [13]. Careful observation revealed that there was a weak band of at 1066 cm^{-1} in sample o, and after the calcination treatment, as directed by the dashed line, the intensity of this band was augmented remarkably in all prepared samples. This result strongly indicated that more amounts of groups identical to that of sample o were created in all prepared samples. Also, for sample b and c, some evident bands of between $420\sim 650\text{ cm}^{-1}$ were clearly displayed which not only indicated the presence of M-O bond [13] but also demonstrated that the compositions of these two samples were similar to each other. This result was well consistent with the XRD results shown in Fig.2b.

3.3 EDS and XPS analysis

To further confirm the element composition of the prepared samples, EDS analysis of all involved samples was carried out and the results are given in Fig.5. For sample o, the peaks assigned to elements of Pb and O were distinctly displayed, and moreover, the atomic ratio of Pb to O was 1: 1.4. This result implied that the industrial lead powder was a lead oxide-based mixture rather than a pure substance of lead monoxide (PbO). While, for sample s, namely, the paste of the SSPLP, the atomic ratio of Pb to O was altered to be 1: 2.3, which was just consistent with the XRD result (pattern s in Fig.2a) that the major component of sample s was PbO_2 . Interestingly, after the calcination process, the carbon element was observed in all prepared samples, and the content of O element in the resultant samples dropped greatly, for example, the atomic contents of O in sample a, b, c and d were, respectively, 66.3%, 52.5%, 46.1% and 40.7%, being rather lower than that of sample s (69.7%). This result substantially demonstrated that most O elements were consumed in the calcination process via the following reactions, $\text{PbO}_2 + \text{C} \rightarrow \text{Pb} + \text{CO}_2$ or $\text{PbO}_2 + \text{C} \rightarrow \text{PbO} + \text{CO}$, implying indirectly that more Pb-based oxides with lower Pb valence state were produced in the final samples.

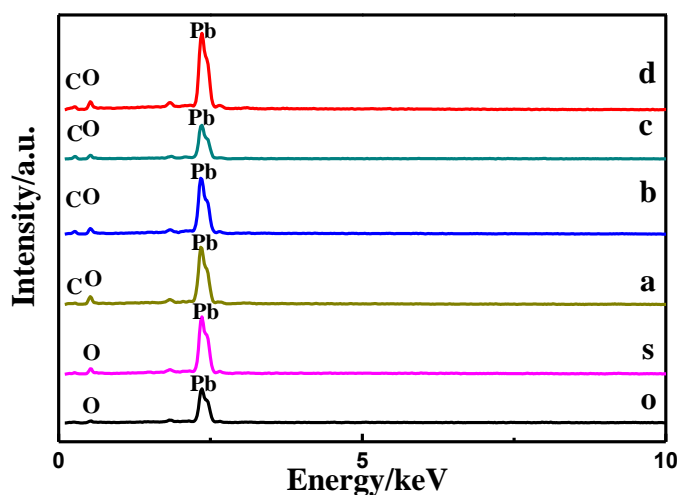


Figure 5. EDS patterns for all the samples. Pattern o, s, a, b, c and d corresponded to sample o, s, a, b, c and d.

Meanwhile, compared to sample s, the atomic content of carbon in the produced samples increased evidently, for instance, the atomic contents of carbon in sample a, b, c and d, respectively, were 13.9%, 26.4%, 35.9% and 44.5%. Generally, the presence of an appropriate amount of carbon in an electrode material was favorable to the electrochemical behavior improvement due to the higher electrical conductivity of carbon itself based on our previous work [14]. Also, the atomic ratios of Pb to O for sample a, b, c and d, were, respectively, 1:3.3, 1:2.4, 1:2.6 and 1:2.8. Thus, it can be, approximately, inferred that more amounts of lead oxides with relatively lower Pb chemical valence were produced in sample b. That is to say, the conclusion that, the compositions of the final samples were different from each other, was again demonstrated by the results of EDS analysis.

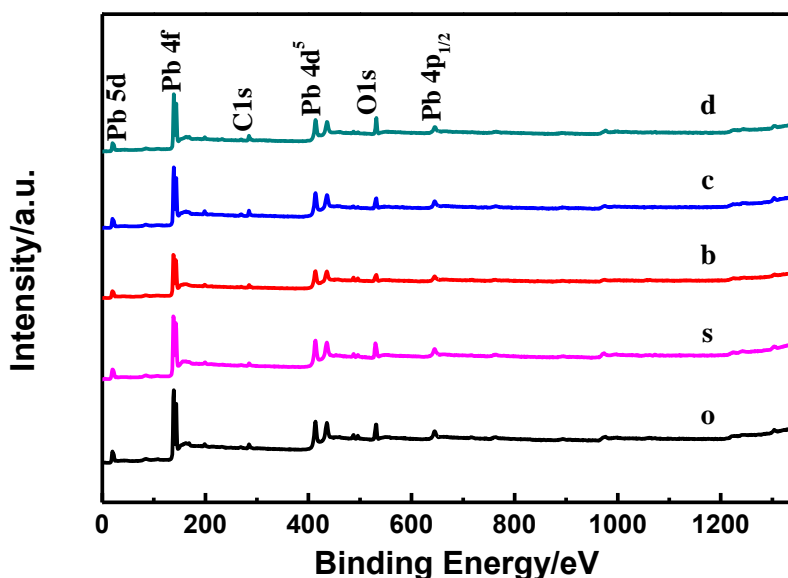


Figure 6a. Wide-scan XPS spectra for the prepared samples. Curve o, s, b, c and d corresponded to sample o, s, b, c and d.

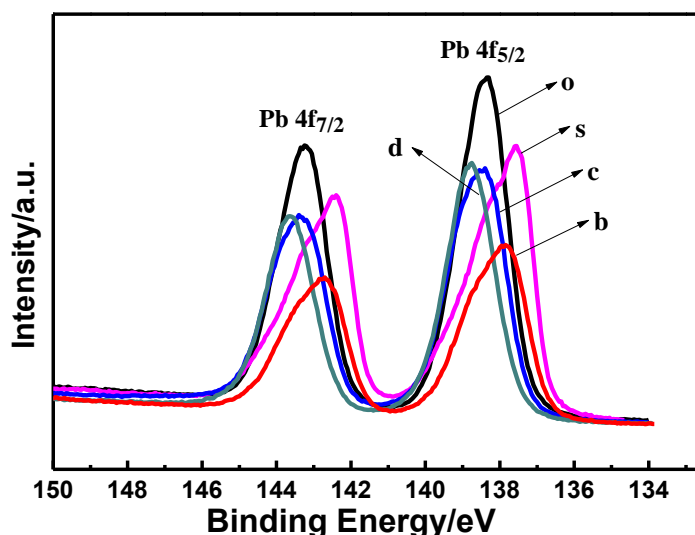


Figure 6b. High resolution XPS spectra of Pb 4f for the samples. Curve o, s, b, c and d corresponded to sample o, s, b, c and d.

To further analyze the valence states of the elements in the synthesized samples, XPS measurements were conducted and the results are illustrated in Fig.6a and 6b. As illustrated in Fig.6a, the results of the wide-scan XPS spectra definitely confirmed the presence of Pb, O and C three elements in the prepared samples which agreed well with the results of EDS analysis (Fig.5). The peak assigned to C element in sample o and s was too small to be observed which suggested that the presence of C in sample o and s was probably due to the adsorption of CO₂ on the surface of both sample s and o. It was reported that the XPS spectrum of Pb4f for the pure PbO nanoparticles could split into two peaks, namely, Pb 4f_{5/2} (137.4 eV) and Pb 4f_{7/2} (141.8eV) peak [15]. And for the metallic Pb, the Pb 4f_{5/2} and Pb 4f_{7/2} peaks were respectively centered at about 136.6 eV and 141.5 eV [16]. Apparently, for all involved samples, the binding energy (BE) of the Pb 4f shifted to higher binding energies compared to the metallic Pb, which strongly suggested that Pb-based oxides were present in all samples [15]. For sample o, the BE energy of Pb 4f_{7/2} (138.26 eV) was slightly smaller than that of Pb 4f_{7/2} (138.3 eV) for Pb₃O₄ [16], and being larger than that of Pb 4f_{7/2} (137.4 eV) for PbO, which effectively demonstrated that sample o was composed of many kinds of Pb-based oxides. While for sample s, the BE energy of Pb 4f_{7/2} (137.5eV) was very close to that of Pb 4f_{7/2} (137.4 eV) for PbO₂ [16], which indicated that the main component of sample s was PbO₂, being consistent well with the results obtained in Fig.2a. Interestingly, the BE values of Pb 4f_{7/2} for sample b, c and d were varied to be 137.8, 138.3 and 138.7 eV, respectively. The higher the carbon black content was, the larger the BE value of Pb 4f_{7/2}. Although the exact value of the valence state of Pb element cannot be determined by the XPS results, the fact that, the carbon black content could significantly affect the chemical valence state of Pb element in the final samples, was confirmed by the XPS results. Or in other words, after the carbon black-present calcination process, most of PbO₂ in sample s were converted into lead oxides with relatively lower Pb chemical valence state.

3.4 Electrochemical performance

Fig.7. shows the discharge profiles of all simulated lead acid batteries assembled by the prepared samples. Evidently, all discharge curves showed a flat voltage plateau at 2.08V which was a marked feature of a lead acid battery based on the former works concerning LABs [17, 18]. The discharge capacities at 0.1C for the lead acid batteries constructed by sample s, o, a, b, c and d were, respectively, estimated to be 109.0, 467.4, 387.5, 458.6, 370.9 and 125.0 mAh. Evidently, compared to the LABs assembled by sample s, the discharge capacities of all the produced samples were significantly promoted. More interestingly, the discharge capacity of sample b was about equal to 98% of the sample o (the fresh industrial lead powder). Thus, above results effectively indicated that carbon black present-calcination process was a feasible and facile method to recover the lead powder from the lead paste of the SSPLP.

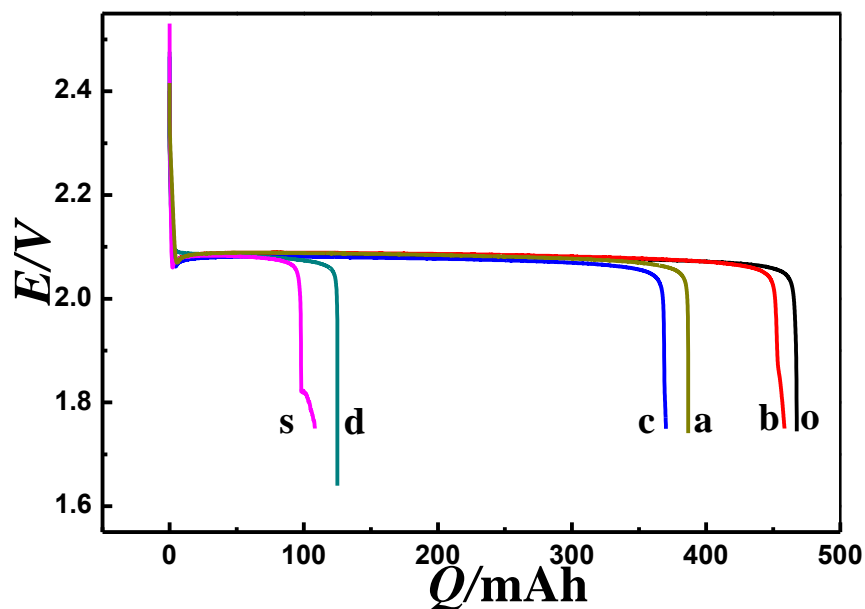


Figure 7. The discharge profiles for the synthesized acid batteries. Curve o, s, a, b, c and d corresponded to the simulated LAB constructed by sample o, s, a, b, c and d. The discharge current rate was 0.1C.

Generally, in the discharging process of a lead acid battery, the formed PbO_2 of the positive lead paste would be converted into PbSO_4 , and in the charging process, the resultant PbSO_4 would be turned into PbO_2 again. As analyzed in the former part of this work, the main component of the SSPLP was $\beta\text{-PbO}_2$. Thus, theoretically, a larger discharge capacity should be delivered by the simulated lead acid battery assembled by sample s. Nevertheless, sample s delivered a very lower discharge capacity. Why? Probably, the following reasons could account for this phenomenon. (1) $\beta\text{-PbO}_2$ with larger particle size and high purity was the main component of sample s. Thus, in the discharging process, the inner parts of a larger $\beta\text{-PbO}_2$ particle cannot react with H_2SO_4 to release PbSO_4 , consequently, a relatively lower discharge capacity was presented by sample s. (2) As seen by the image o in Fig.3b, the fresh positive lead paste had a space-framed structure which was very favorable to the flowing of the H_2SO_4 electrolyte. And in the case of sample s (image s in Fig.3b), $\beta\text{-PbO}_2$ particles were densely packed together in which the amounts of the passageways for the flowing of the H_2SO_4 electrolyte were limited as compared to the case of sample o. Therefore, sample s showed a lower discharge capacity. Thus, another problem came into being. What was the preparation process of the larger $\beta\text{-PbO}_2$ particles? Generally speaking, after the formation process, most parts of the raw lead paste of the positive lead plate were converted into PbO_2 (as shown by the first orange yellow particle, particle 1 in Fig.8), and in the discharging process, most PbO_2 reacted with H_2SO_4 to form the PbSO_4 (gray part of particle 2), and probably, in this case, some inner parts of PbO_2 particle remained unreacted leading to the formation of a small core consisting of pure PbO_2 (as shown by orange yellow part of particle 2).



Figure 8. The possible diagram of the formation process for the larger PbO_2 particle of the SSPLP.

And, after the next charging process, the formed PbSO_4 again were totally converted into PbO_2 forming a larger PbO_2 particle (as shown by particle 3). And, in the next discharging process, some unreacted PbO_2 were created again, to and fro, PbO_2 particles with a larger size were produced (as shown by orange yellow and the yellow part of particle 4). Lastly, more amounts of larger and closely packed PbO_2 particles were produced leading to the formation of the SSPLP. That is to say, the overcharging was the main reason which produced the issue of SSPLP.

4. CONCLUSIONS

In this study, for the first time, a very simple method of carbon black present-calcination was developed to recover the lead powder from the lead paste of the SSPLP. The results of XRD and XPS strongly indicated that the main component of the SSPLP was $\beta\text{-PbO}_2$, and after the calcination treatment, Pb-based oxides with relatively lower Pb chemical valence states were generated. SEM images suggested that the content of carbon black was an important factor which greatly influenced the morphologies of the final samples, and after the calcination process, more cylinder-shaped particles were produced in sample b. Most importantly, the results of the battery performance measurement effectively demonstrated that the discharge capacity of sample b was almost 98% of the fresh industrial lead powder. That is to say, the newly developed method of carbon black present-calcination can be employed to recover the lead powder from the lead paste of the SSPLP, which is very meaningful to the cyclic utilization of lead acid battery, as well as being favorable to the environmental protection.

ACKNOWLEDGEMENTS

This work was supported by National Natural Science Foundation of China (21676022 & 21706004) and the State Key Program of National Natural Science of China (21236003), and the Fundamental Research Funds for the Central Universities (BHYC1701A & JD1701). This work was also financially supported by the Natural Science Foundation of Hebei Province of China (No. B2015205150) and the Technical Innovation Advanced Research Foundation of Hebei Normal University (L2018K03).

References

1. H. Xia, L. Zhan and B. Xie, *J. Power Sources*, 341 (2017) 435.
2. L.K. Liu, L. Liu, Z.X. Chen, J.X. Wang, Z.J. Zhou, Y.J. Zhang, M.Y. Wang, Y.F. Zhang and K.Q. Ding, *Chin. Labat Man*, 50 (2013) 99.

3. G. Fusillo, D. Rosestolato, F. Scura, S. Cattarin, L. Mattarozzi, P. Guerriero, A. Gambirasi, N. Brianese, P. Staiti, R. Guerriero and G. La Sala, *J. Power Sources*, 381 (2018) 127.
4. T.W. Ellis and A.H. Mirza, *J. Power Sources*, 195 (2010) 4525.
5. J. Pan , Y. Sun, W. Li, J. Knight and A. Manthiram, *Nat. Commun.*, 4 (2013) 2178.
6. M. Volpe, D. Oliveri, G. Ferrara, M. Salvaggio, S. Piazza, S. Italiano and C. Sunseri, *Hydrometallurgy*, 96 (2009) 123.
7. T.W. Ellis and A.H. Mirza, *J. Power Sources*, 195 (2010) 4525.
8. J. Pan, X. Zhang, Y. Sun, S. Song, W. Li and P. Wan, *Ind. Eng. Chem. Res.*, 55(2016) 2059.
9. Y.R. Bian, L. Liu, Z.X. Chen, L.K. Liu, M.Y. Wang, Y.J. Zhang, Y.J. Zhang and K.Q. Ding, *Chin. Labat Man*, 50 (2013) 275.
10. L. Liu, L.K. Liu, Z.X. Chen, C.B. Zheng, J.X. Wang, Z.J. Zhou, M.Y. Wang, Y.J. Zhang, Y.F. Zhang and K.Q. Ding, *Chin. Battery Ind.*, 18(2013) 58.
11. K. Ding, Y. Wang, H. Yang, C. Zheng, Y. Cao, H. Wei, Y. Wang and Z. Guo, *Electrochim. Acta*, 100 (2013) 147.
12. W. An, J. Fu, J. Su, L. Wang, X. Peng, K. Wu, Q. Chen, Y. Bi, B. Gao and X. Zhang, *J. Power Sources*, 345 (2017) 227.
13. K. Ding, J. Zhao, J. Zhou, Y. Zhao, Y. Chen¹, Y. Zhang, B. Wei, L. Wang and X. He, *Int. J. Electrochem. Sci.*, 11 (2016) 446.
14. K. Ding, Y. zhao, L. Liu, Y. Li, L. Liu, L. Wang, X. He and Z. Guo, *Electrochim. Acta*, 176 (2015) 240.
15. H. Sivaram, D. Selvakumar, A. Alsalmé, A. Alswieleh and R. Jayavel, *J. Alloys Compd.*, 731 (2018) 55.
16. N. Comisso, L. Armelao, S. Cattarin, P. Guerriero, L. Mattarozzi, M. Musiani, M. Rancan, L. Vázquez-Gómez and E. Verlato, *Electrochim. Acta*, 253 (2017) 11.
17. Y.Y. Chen, M. Zhao, J. Zhao, Y.J. Zhang, Y. Li, Z.X. Chen, M.Y. Wang and K.Q. Ding, *Chin. Labat Man*, 53 (2016) 1.
18. B. Hong, L. Jiang, H. Xue, F. Liu, M. Jia, J. Li and Y. Liu, *J. Power Sources*, 270 (2014) 332.